Hotta *et al. ROBOMECH Journal* (2023) 10:2
https://doi.org/10.1186/s40648-023-00240-4

ROBOMECH Journal

**RESEARCH ARTICLE** **Open Access**

# Lightweight underwater robot developed for archaeological surveys and excavations

Shohei Hotta[1], Yusuke Mitsui[1], Mizuki Suka[2], Norimitsu Sakagami[2*] and Sadao Kawamura[1]

**Abstract**

This paper reports the development of a lightweight remotely operated vehicle that performs underwater excavation work for archaeological surveys. Discovering underwater artifacts is generally difficult because they are in high risk areas and are often covered with sediment. To discover them, divers and large remotely operated vehicles must conduct excavation work with a manipulator(s). Nevertheless, accomplishing such tasks is difficult for small and portable underwater robots without a manipulator(s). As described herein, we developed a lightweight underwater robot of 35 kg that can remove sediment from the seabed or lake bottom using its thrusters instead of a manipulator. Numerous redundant thrusters are equipped with the robot to compensate the reaction force of the thrusters for sediment removal. Eight thrusters are arranged not only for sediment removal but also for fine maneuvering. First, through preliminary experiments, we investigated the potential use of a water flow generated using a pair of small marine thrusters to remove surface sediment. Next, we described the design and development of a lightweight underwater robot with eight thrusters and high-definition cameras for archaeological surveys. Finally, we conducted field experiments to demonstrate the sediment removal performance and usefulness of the developed robot.

**Keywords** Remotely operated vehicle, Underwater archaeological survey, Underwater excavation

## Introduction

Underwater archaeological survey and investigation involves searching for sites, recording sites, excavation, and many other tasks. First, non-destructive survey methods are applied for research activities. Although *in situ* preservation is the first option [1], excavation of sites and/or recovery of archaeological materials are conducted for scientific studies if appropriate.

For archaeological non-destructive and non-intrusive surveys, autonomous underwater vehicles (AUVs) and remotely operated vehicles (ROVs) are used, offering highly efficient operations in deep water and in high risk areas. The literature [2] reports studies conducted using the *C-Surveyor I* AUV to investigate deep-water shipwrecks in the Gulf of Mexico. The *C-Surveyor III* AUV collected multibeam bathymetry data and digital still images to create the photomosaic for better understanding the archaeological site. The compact AUV *Girona 500* (140 kg) collected stereo images to create a 2.5D textured model and 3D reconstruction of the ship wreck site *La Lune* for subsequent archaeological investigation [3]. As pre-disturbance investigation tools, other AUVs were used to acquire optical images of archaeological sites for 3D reconstructions, e.g. [4, 5]. In addition to AUVs, ROVs are used for pre-disturbance investigations intended to capture images and to produce 3D models of archaeological sites. The ROV *Minerva* investigated a sunken ship projecting upward about 10 m from the seabed [6]. During the investigation, an archaeologist evaluated the images while giving feedback about their quality. For deep-sea archaeology, the research team conducted the ROV 3D project [7] in which the main goal was to create a high-resolution 3D model of the site and visualize

---

*Correspondence:
Norimitsu Sakagami
sakagami@tokai.ac.jp
[1] Department of Robotics, Ritsumeikan University, Kusatsu, Japan
[2] Department of Marine Science and Ocean Engineering, Tokai University, Shizuoka, Japan

the surveyed part of the site in real-time for the operator. Visualization allows the operator to ensure complete coverage of the interesting area. The real-time feedback is one important feature of ROVs. The vehicles described above contribute to archaeological surface surveys with non-destructive techniques and without contact artifacts.

After non-destructive detailed surveys and careful consideration, excavation and/or recovery of archaeological material may be conducted. At dangerous sites for humans, large and heavy ROVs with manipulators have been used to carry out such contact work. In the Skerki Bank Project [8], the ROV *Jason* excavated an archaeological site using the robotic arm with an excavation tool. *Jason* grasped and recovered archaeological objects using the arm controlled by an operator while hovering automatically above the site. In the Tortugas project [9], the ROV *Merlin* (3 tons) was equipped with manipulator arms, a limpet suction recovery device, and the Sediment Removal and Filtration system (SeRF) to excavate the Tortugas shipwreck site and recover artifacts using the manipulators. The SeRF, which is driven by a high-horsepower water pump, was designed to recover small artifacts during sediment removal. Unnecessary sediment is displaced from the excavation site. Small artifacts are captured in the container. In the project [10], the work-class ROV was equipped with an excavation system. The ROV removed the sediment from the excavation area using the system, and lifted several artifacts to the surface using a 7-function manipulator arm. In addition to these, the ROV *Hercules* had an excavation toolkit used by the manipulators to dig and remove sediment and recover artifacts in the deep sea [11]. These excavation and recovery systems are devices that use suction force generated by the water flow.

In recent years, underwater robots of new types, differing distinctly from the conventional ROVs described above, have been developed and tested for underwater archaeological excavation and recovery. The Crabster CR200 (600 kg) underwater walking robot has six legs, two of which are used as the manipulators [12]. The robot was tested to recover imitation artifacts using the manipulator arms in a sea trial. The experiment was successful. *Ocean One* [13], an underwater robotic avatar (200 kg), has manipulators and tendon-driven grippers to accomplish underwater work for archaeological surveys. The gripper stiffness can be adjusted to accommodate delicate and hard objects. *Ocean One* recovered an artifact from a deep-sea archaeological site using the manipulators [14]. Although these robots have no special suction tools, their experiments demonstrated the great potential of underwater robots for underwater recovery and excavation.

Considering actual operations of the above large and heavy underwater robots, a large support vessel with a winch for launch and recovery is necessary for conducting research activities. However, it is often the case that, because of equipment and budget constraints, only small boats without a launch-and-recovery system are used for research surveys. In such cases, archaeological sites must be investigated by scuba divers and/or portable underwater robots. If the site of interest is at a dangerous depth for humans, then the only method of investigation is to use a portable underwater robot for archaeological surveys. Although pre-disturbance surveys by small underwater robots have been used [15, 16], no report of the relevant literature describes portable robots with excavation tools to investigate archaeological sites that are covered by sediment.

In this report, we propose a portable underwater robot having redundant quantities of thrusters used for sediment removal. Several conventional methods are used today for sediment removal such as a water dredge, prop-wash, and water jet [17]. Although water dredges, which use suction force generated from water flow, are proven and promising devices, mounting a high-pressure water pump and a manipulator to handle its intake port greatly increases the mass and size of an underwater robot. The approach using thrusters proposed herein is similar to the idea of prop-wash and water jet in the sense of using the stream of water that is blown out. The prop-wash uses a vessel's propeller and a right-angle tube for directing its propeller thrust downward to remove large amounts of sand from the site. However, this approach is usually extremely destructive to archaeological surveys because controlling the water flow properly and narrowing down the area of excavation is extremely difficult. The water jet is used only to a limited degree for archaeological investigations because it generates a long-range water stream and because it worsens visibility at silty or sandy sites. For the proposed method, two regular marine thrusters are installed so that two water streams generated by the thrusters strike each other. The water flow speed increases at the point where the two water streams intersect. However, the water flow speed in other areas is reduced because of the energy loss which occurs after the water streams strike each other.

For this work, we develop a lightweight underwater robot (Fig. 1) that can remove sediment on the sea or lake bottom using its thrusters instead of manipulators. To achieve sediment removal in the minimum area of interest, we first determine the configuration of two marine thrusters through preliminary experiments to measure the water flow speed distribution and force generated by the thrusters. After determining the two thruster configuration for sediment removal, we also determine the configurations of other thrusters for our underwater robot based on numerical analysis. The thruster configurations

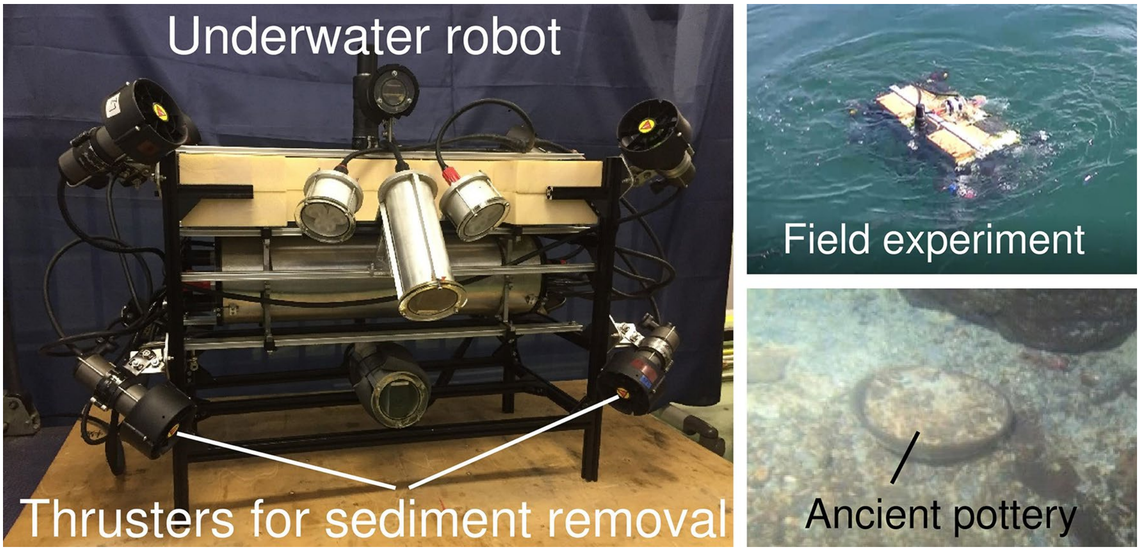

**Fig. 1** The developed underwater robot and ancient pottery discovered by this robot during non-destructive survey. The pottery was covered with some sediment

allow our underwater robot to remove sediment in the minimum area of interest. As a result, all the thrusters installed on the developed robot are useful not only for removing sediment for underwater excavation but also for fine maneuvering of the robot when external disturbances occur. Additionally, we conducted field experiments at Lake Biwa to demonstrate the performance of the developed robot.

This paper is organized as follows. "Preliminary experiment for sediment removal using thrusters" section explains preliminary experiments conducted to assess the effectiveness of small regular thrusters for removing sediment. "Numerical analysis" section presents our numerical analyses of a thruster configuration for an underwater robot to realize underwater maneuvering and excavation work. The design and development of the small underwater robot with eight thrusters are presented in "Design and development of the underwater robot" section. "Field experiment" section describes results of field experiments conducted in Lake Biwa using a small fishing boat. The performance of the developed robot and sediment removal were evaluated. Finally, future work and conclusions are presented in "Future work" and "Conclusion" sections.

## Preliminary experiment for sediment removal using thrusters

We use small regular thrusters to remove sediment on the sea or lake bottom for underwater surveys. This section presents measurement results of the water flow speed and force generated by the thrusters to determine the thruster configuration of our underwater robot.

### Experiment setup for preliminary experiments

This experiment was conducted to determine a thruster configuration that can produce a water flow peak at a place of interest. We assume that two thrusters are used to generate water flow for sediment removal. We measured the steady-state water flow distributions and forces generated by commercial marine thrusters (LBT100; Seabotix Inc.). Figure 2 portrays the experiment setup. A pair of the thrusters was fixed to a metal frame and was installed in a water tank. The distance between the two thrusters was set as 700 mm. The water tank depth was 1 m. The thrusters were installed horizontally at 0.5 m depth. Three thruster angles of 30°, 45°, and 60° were tested to find a thruster configuration able to produce strong water flow in a partial area The thruster angle was 45° in Fig. 2. The origin of the coordinate system coincides with the point at which the extended lines of the central axes of the two thrusters intersect. A water flow sensor was used to measure the water flow speed at 280 points to evaluate the water flow distribution. We changed the position of the sensor 280 times. Each measurement was conducted during 10 s to calculate the average water flow. A force sensor was used to measure the forces generated by the thrusters. A metallic plate attached to a force sensor was placed in the water tank as shown in Fig. 2. We prepared three plates to which force is applied: $0.1 \times 0.1$, $0.2 \times 0.2$, and $0.3 \times 0.3$ $\mathrm{m}^2$. They

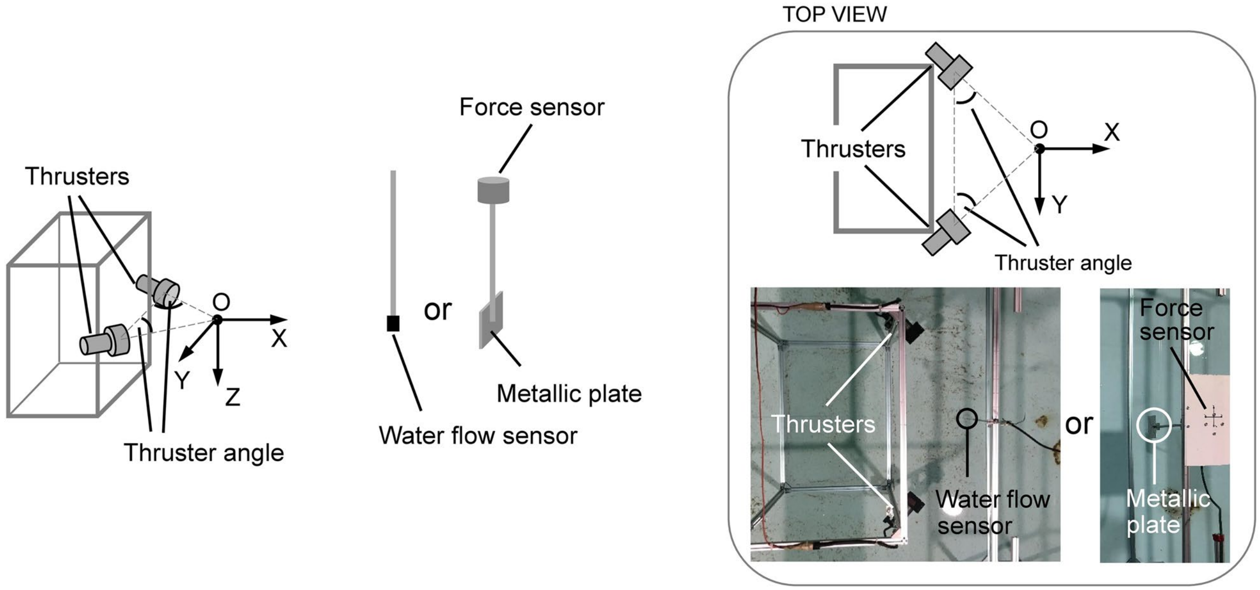

**Fig. 2** Experiment setup for water flow and force measurements. The origin is set at the intersection of the extension lines of the central axes of the two thrusters

were placed on the $x$—axis at positions from $-0.1$ to 0.6 m. Each measurement was conducted during 10 s to calculate the average force.

### Water flow distribution

Figure 3 presents the horizontal distributions of the steady-state water flow for thruster angles of 30°, 45°, and 60°. Blacker areas in the figure had faster water flow. The middle images for each thruster angle show the water flow distribution on the $x-y$ plane. Figure 4 depicts the vertical distributions of the water flow. As indicated from these results, at thruster angles of 30 and 45 degrees, clear water flow peaks are apparent near origin O: the intersection of the extension lines of the central axes of the two thrusters. These thruster configurations are expected to help remove sediment in a minimum area of interest. However, no clear water flow peak is apparent at the thruster angle of 60°.

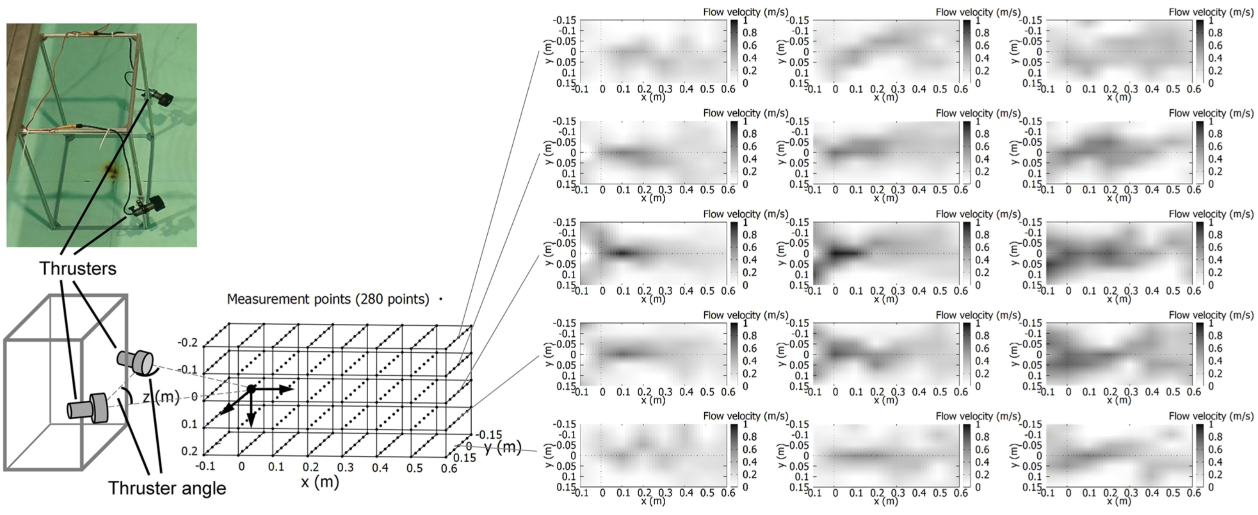

(c) Thruster angle 30 (deg) (a) Thruster angle 45 (deg) (b) Thruster angle 60 (deg)

**Fig. 3** Experiment results showing the steady-state water flow distribution using two thrusters. Results show the horizontal distribution at three thruster angles

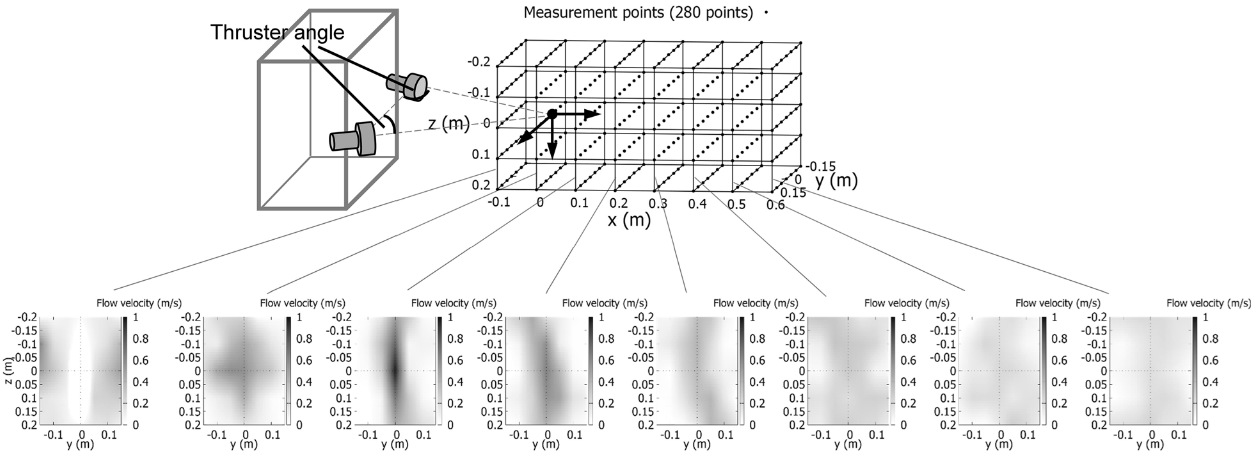

(a) Thruster angle 30 (deg)

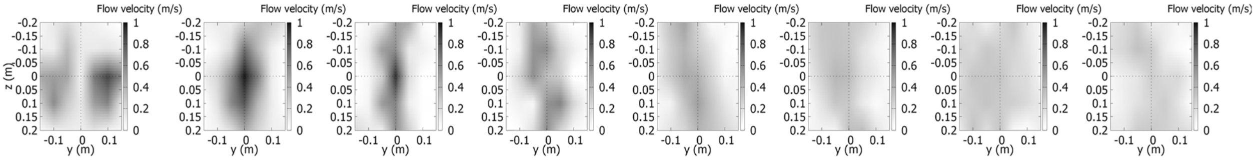

(b) Thruster angle 45 (deg)

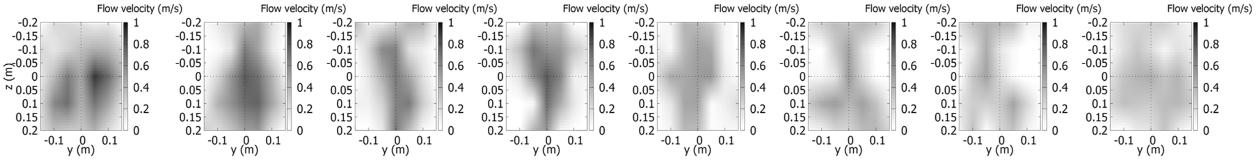

(c) Thruster angle 60 (deg)

**Fig. 4** Experiment results show the vertical distribution for three thruster angles

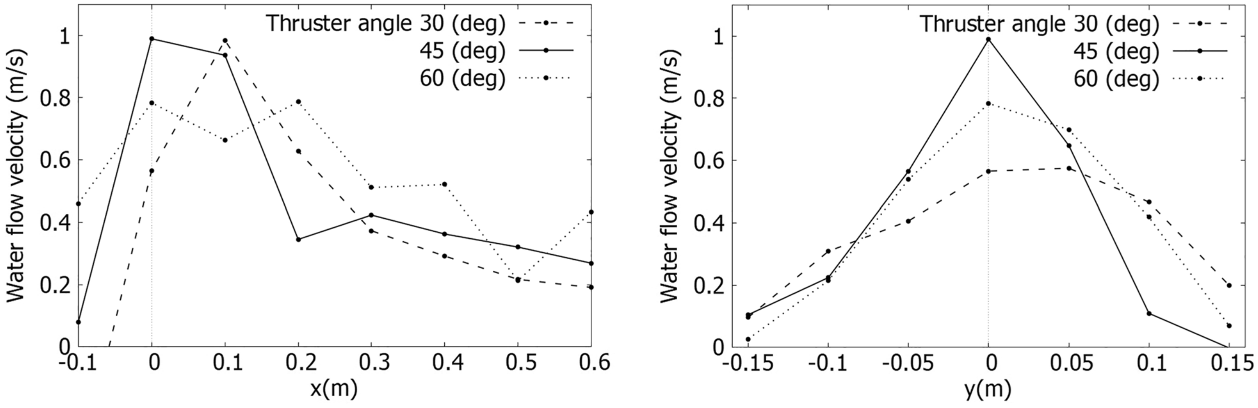

**Fig. 5** Experiment results found for the water flow speed. The left panel shows the water flow speed along the x-axis. The right panel shows that along the y-axis

Two graphs presented in Fig. 5 show water flow speeds along the $x$–axis and $y$–axis for three thruster angles of 30°, 45°, and 60°. These experiments indicated that the maximum water flow speed near the origin is about 1.0 m/s at the thruster angle of 45°. The water flow speed decreases rapidly in areas other than the origin at 45°. Henceforth, we adopt the thruster angle of 45° for our underwater robot.

### Force measurement

We also measured the force generated by the thrusters installed at 45° to check whether excessive force is applied to artifacts. As shown in Fig. 2, a metallic plate attached to a force sensor was placed in the water tank to measure the force. The left panel of Fig. 6 portrays the experimentally obtained results of the force generated by the thrusters acting on the plate. The right panel shows the numerical results converted to pressure using the plate area. Results show that force of 13 N or less and pressure of 460 Pa or less works near the origin.

The estimated bending strength of the Jomon pottery when it was made was more than 2 MPa [18]. Compared to this value and sizes of the Jomon pottery, the bending moment resulting from the measured force or pressure is very small. Therefore, it is unlikely that the Jomon pottery would be damaged by this method even if the artifacts were fragile.

### Sediment removal test

We conducted an experiment designed to test the sediment removal performance of the two thrusters. The thrusters were fixed at the thruster angle of 45° and the distance between the thrusters was set as 700 mm, as described above. Also, as presented in Fig. 7, the thrusters were tilted downward 45° because, to prevent suction of gravel, sand, etc., the thrusters cannot be placed at the same height as artifacts on the seabed or lake bed. As illustrated in Fig. 7, the distance between the straight line connecting the two thrusters and the point where the two water streams intersect was set as 350 mm.

When water flow strikes on the seabed or lake bed because of the thruster tilt, the energy of the fluid is lost. Moreover, the sediment might not be removed. Therefore, we conducted a test to assess the possibility of removing sand covering underwater pottery. Instead of using natural sediment, we used commercially available sand. For the test, we prepared two pottery samples: a 462 g plate with 1.87 specific gravity and a 229.5 g pot with specific gravity of 2.05. After the plate and pot had been buried in the sand, we attempted to remove the covering sand by adjusting the thrust force

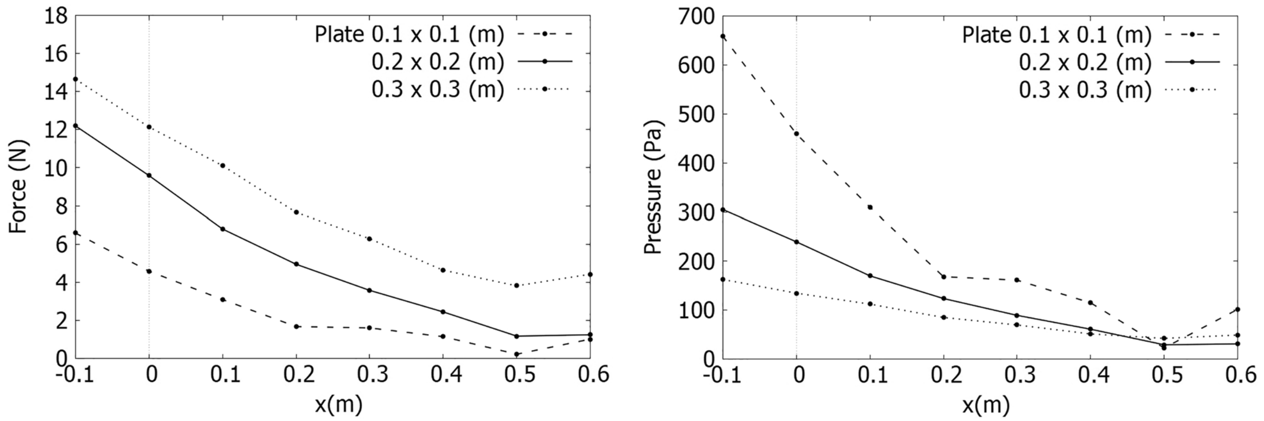

**Fig. 6** Experimentally obtained results indicating the measured force and pressure acting on the plates

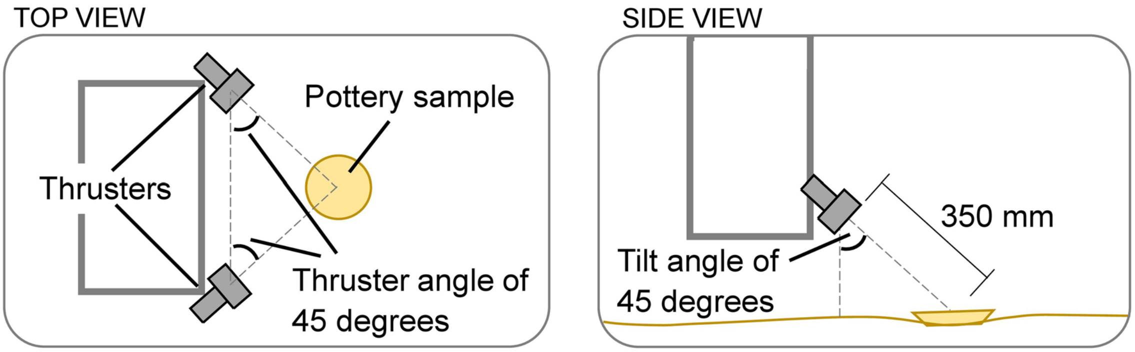

**Fig. 7** Experimental setup for sediment removal test

**Fig. 8** Sediment removal test for a plate

**Fig. 9** Sediment removal test for a pot

output using joystick operation. We removed the sediment using the thrusters, as shown in Figs. 8 and 9.

These experiments demonstrated that the thrusters used here have sufficient capacity to remove sediment.

## Numerical analysis

In the preceding section, we demonstrated experimentally that two thrusters can be used for sediment removal. This section presents a numerical assessment of the thruster configuration used for the underwater robot. This section presents an assessment of the robot movement in all directions.

### Force generated by thrusters for maneuvering

We propose a thruster configuration for an underwater robot, as portrayed in Fig. 10. The robot has eight thrusters. Figures 10 and 11 present the physical parameters in this numerical analysis. For static analyses, we consider only thrust forces.

We numerically estimate the resultant force $\mathbf{f}_r$ when thrust forces $f_1, f_2, \cdots, f_8$ are output in the range of $-21.56 \le f_i \le 21.56$ N (the maximum thrust forces of the respective thrusters installed on our robot are 21.56 N) under the constraint condition that the rotational moment $\boldsymbol{\tau}_r$ acting on the robot generated by the thrusters is zero. The resultant force $\mathbf{f}_r$ can be given as

$$\mathbf{f}_r = \mathbf{T}_1\mathbf{f}$$

when $\boldsymbol{\tau}_r = \mathbf{T}_1'\mathbf{f} = 0$. Therein, $\mathbf{f} = \left(f_1, \cdots, f_8\right)^T$. $\mathbf{T}_1$ and $\mathbf{T}_1'$ are the thruster configuration matrices given by the thruster positions and angles in Figs. 10 and 11. A sequential search algorithm was used to find the set of resultant forces by changing the magnitude and direction of the force $\mathbf{f}$. Figure 12 portrays the direction and magnitude of the resultant force generated by the eight thrusters. The upper right figure illustrates a three-dimensional representation of the set of the resultant forces. The other figures show front, side and top views of the set of the resultant forces. Based on the result, the eight thrusters with the configuration can output the resultant forces of 86.24 N in the $x$ and $z$ directions, and 121.52 N in the $y$ direction for the robot. From this result, we use the thrust force in the $y$ direction for long-distance travel and the thrust force in the $x$ direction during visual survey.

Because the thruster configuration is symmetric in the $x-y$, $x-z$, and $y-z$ planes, the other thrusters can compensate the reaction force from the thrusters used for sediment removal.

## Design and development of the underwater robot

This section presents the design and development of an underwater robot to conduct excavation work and to provide fine maneuvering near a lake bottom using thrusters.

### Underwater robot *MIKAN*

We designed and developed the ROV *MIKAN*, as shown in Fig. 13 [19]. The overall system, which is 950-mm-wide, 550-mm-long, and 750 mm high, weighs approximately 35 kg in air. It has neutral buoyancy in water. This robot's eight thrusters can produce surge, heave, sway, and yaw motions of the system. The redundant number of the thrusters is useful for the robot to conduct excavation

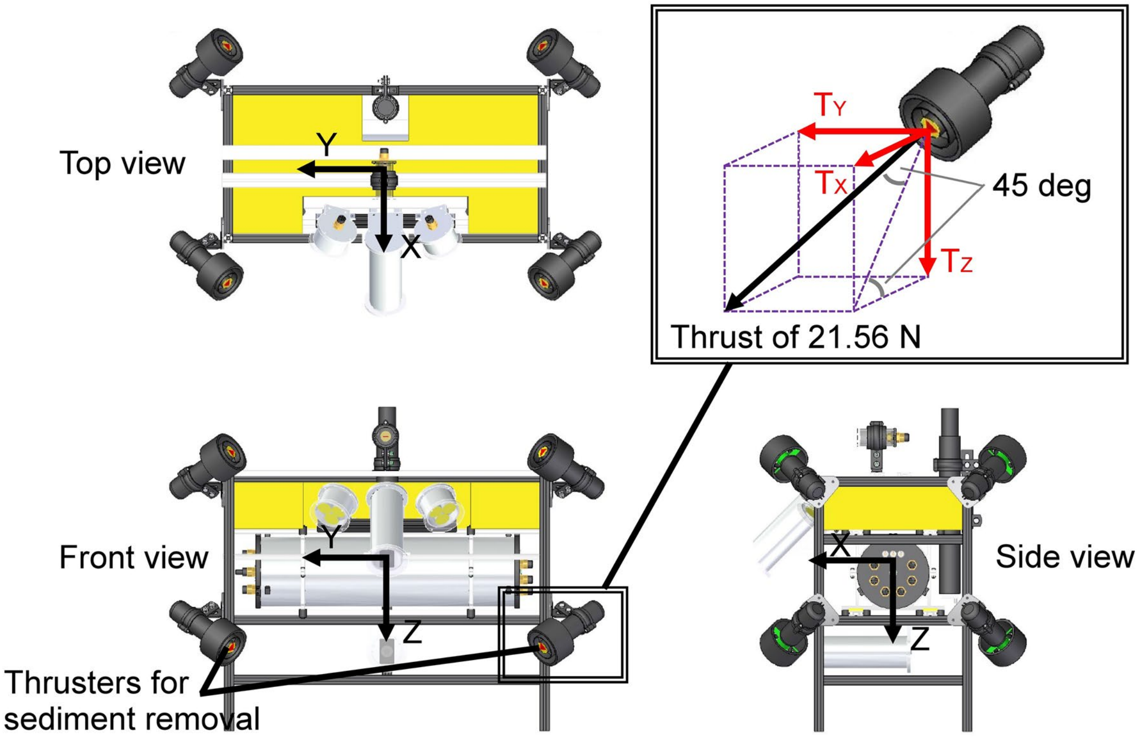

**Fig. 10** Thruster configuration

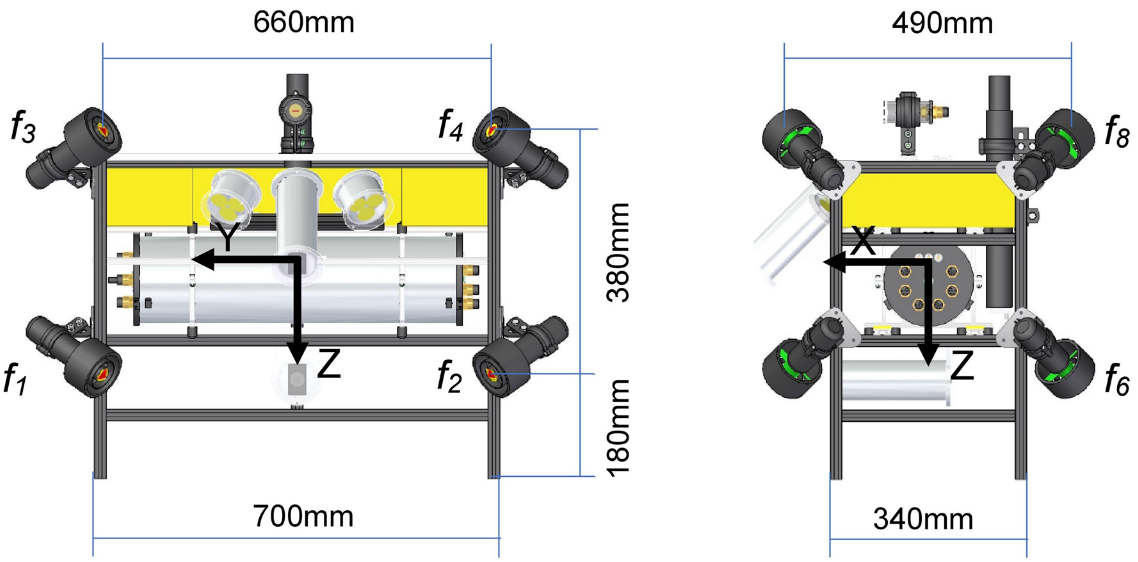

**Fig. 11** Physical parameters. Thrusters that generate forces of $f_5$ and $f_7$ N are located respectively behind the first and third thrusters ($f_1$ and $f_3$)

work, stabilize its body, and realize good maneuvering in water-flow environments. Two high-definition video cameras installed at the top and bottom of the robot record artifacts found underwater. The cameras enable to an operator to acquire the three-dimensional information of the artifacts. The images which are obtained are also useful to create a three-dimensional model using photogrammetry. The robot has an acceleration sensor, digital compass, depth sensor, water sensor and a Super Short Baseline (SSBL) acoustic positioning system, which can

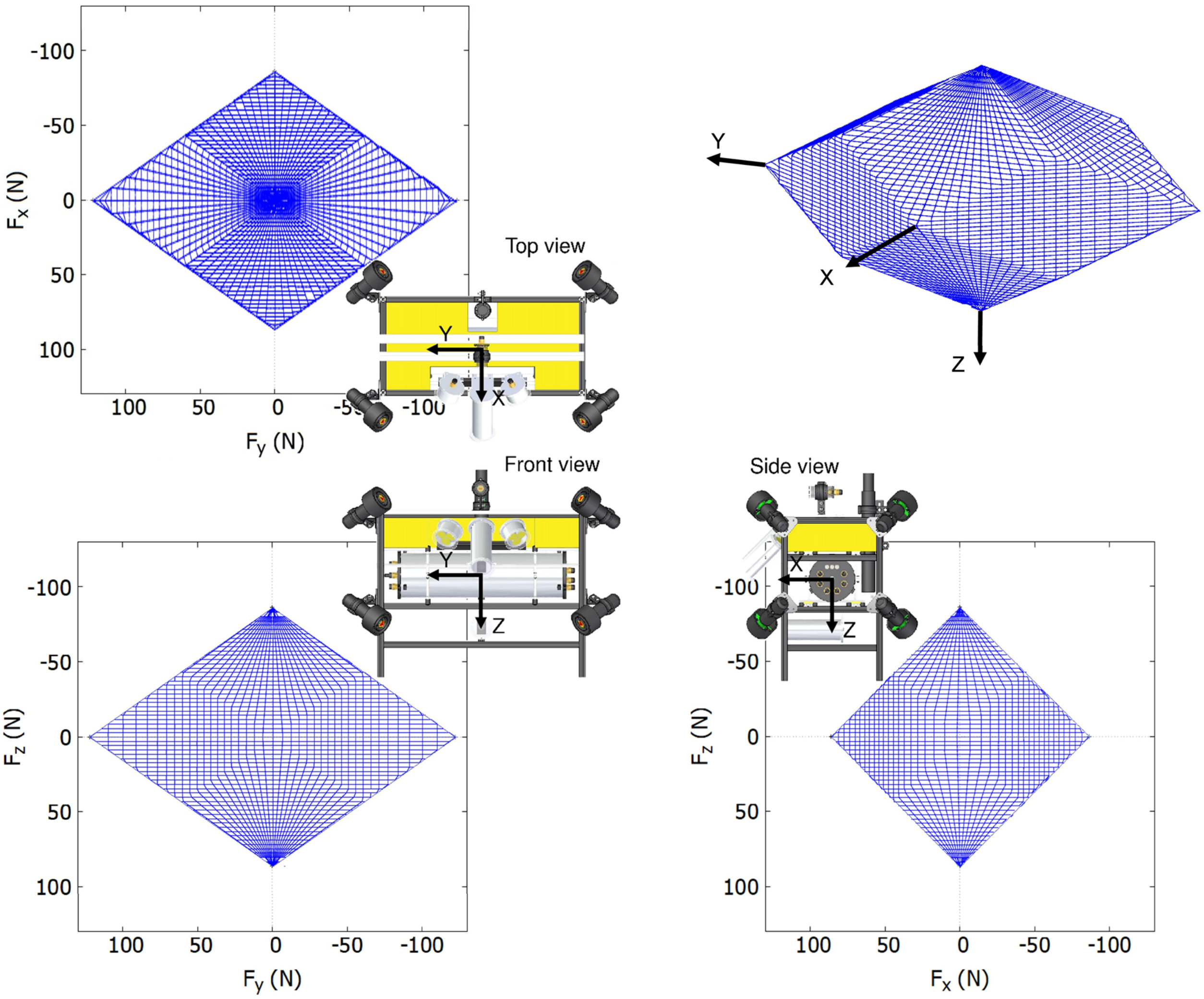

**Fig. 12** Thrust force for maneuvering (using eight thrusters)

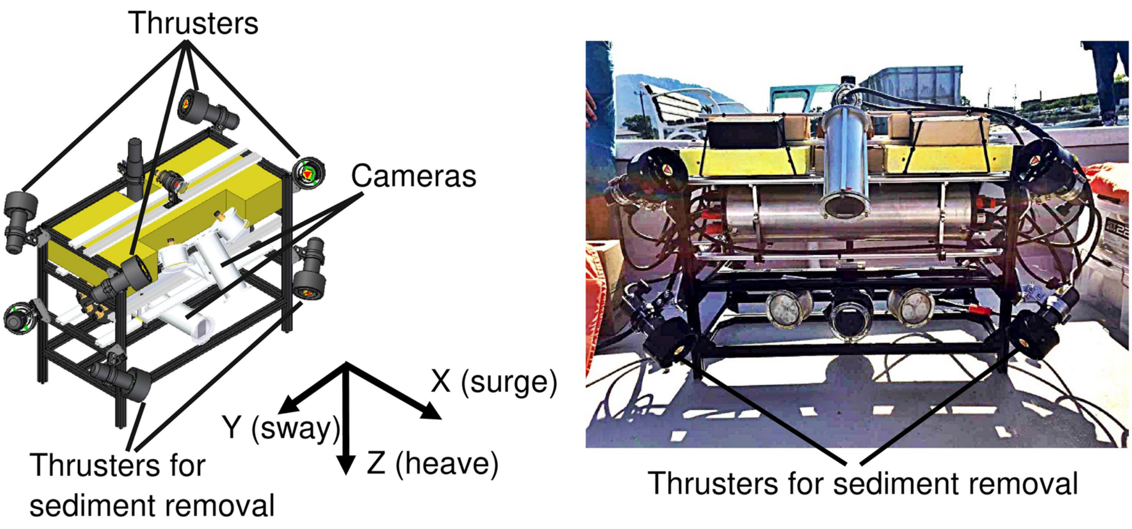

**Fig. 13** CAD and the developed robot

calculate the global position by combining GPS data and the relative position of the robot with respect to a support boat.

Before conducting field experiments, we evaluated the motion speed by measuring the travel distance and time at a water tank. The respective speeds of surge, sway, and heave were approximately 0.31, 0.60, and 0.67 m/s. The angular speed of the yaw was 118 deg/s.

### Thruster configuration and control devices

We adopted the eight-thruster configuration based on results of preliminary experiments and numerical analysis. As shown in Fig. 10, the thruster configuration is symmetric in the $x - y$, $x - z$, and $y - z$ planes. The maximum thrust forces of the respective thrusters are 21.56 N. The eight thrusters can output total force of 86.24 N in the $x$ and $z$ directions, and 121.52 N in the $y$ direction for the robot. The configuration can generate force in any direction. Particularly, the force of the $y$ direction is stronger than the other direction forces. For that reason, the robot can swim as fast as possible for archaeological surveys near the sea or lake bottom. The two thrusters attached to the lower part of the front generate sufficient force to remove sediment. The other thrusters are used to cancel the thrust force for sediment removal.

During visual observations, the robot lands on the lake bottom completely. Vertical thrust force in the $z$ direction is used for position stability on the bottom. The force in the $z$ direction presses the robot body against the bottom so that it does not move under the disturbance. The pressing force stabilizes the robot position and posture. The resultant stability helps to acquire clear images of artifacts.

The developed robot is controlled using a control device that has two joysticks and two potentiometer dials, as presented in Fig. 14. One direction (white arrow in Fig. 14) of one joystick is assigned to blow off sediment and achieve sediment removal.

## Field experiment

To test the sediment removal and robot motion performance, we conducted a field experiment at Lake Biwa using the underwater robot with the sediment removal thrusters. The field experiment setup is presented in Fig. 15.

### Sediment removal and robot motion performance

Using the developed robot, we conducted sediment removal testing at a depth of around 50 m. The water flow from the two front lower thrusters was adjusted using joystick operations to remove the sediment and thereby expose several rocks, as portrayed in Figure 16. They were initially covered with some sediment, as shown on the left side of Fig. 16. Figure 16a, b show photographs of lake bottom rocks taken when we conducted sediment removal. Figure 16c shows a small stone on the lake bottom during sediment removal. It is apparent from the findings and observations that the sand only around the stone had been removed and that the bottom of the lake was exposed. Figure 16d shows the bottom rocks including a stone with a shape similar to that of a plate. As this figure shows, part of the sand around the stone and in the stone was blown away by the water flow generated by

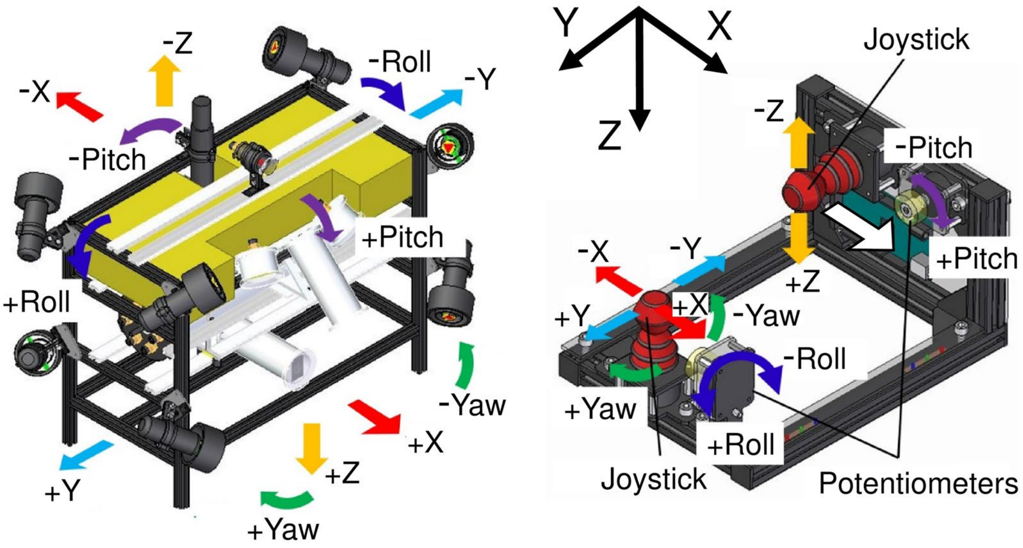

**Fig. 14** Control device for the developed robot

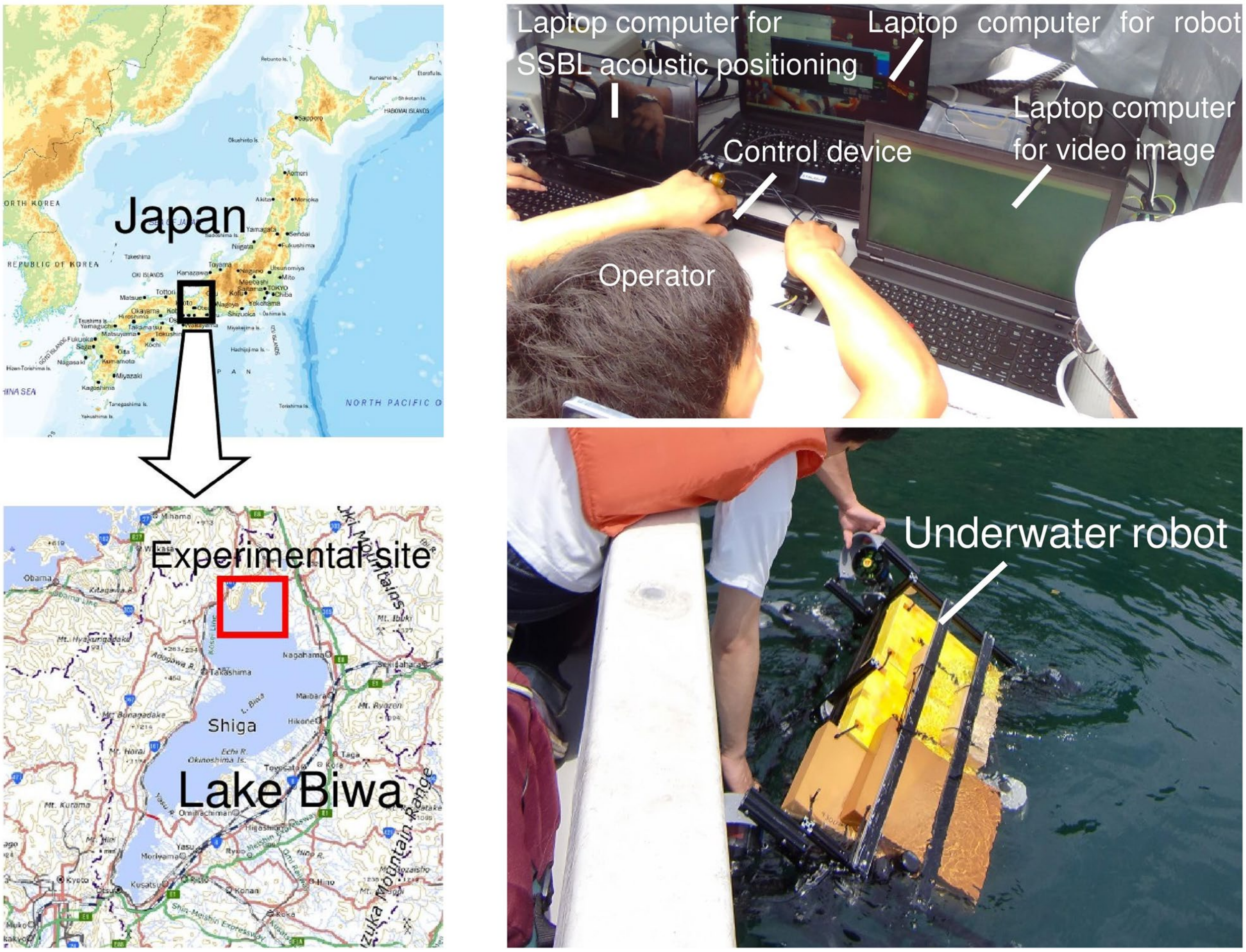

**Fig. 15** Experiment setup (Map based on the Digital Map (Basic Geospatial Information) published by Geospatial Information Authority of Japan)

the thrusters. After blowing off of the sediment, we visually recognized the exposed objects clearly. This function is expected to be helpful for small underwater robots to excavate an archaeological site.

We obtained data from the several sensors to evaluate the robot motion performance. Figure 17 shows the depth data obtained when the robot dove directly into the lake bottom from the water surface. As the figure shows, the robot moved to a depth of about 70 m in 270 s. Therefore the dive speed was approximately 0.26 m/s which was slower than that measured in a water tank. This was due to the influence of the tether cable tension and external disturbance.

Figure 18 presents the underwater position of the robot measured using the SSBL acoustic positioning system during an archaeological pre-disturbance survey. Although the support boat drifted about 100 m because of the influence of wind and water flow, the robot remained at a depth of about 58 m at the 50 $m^2$ lake bottom. There the survey was conducted by the operator via remote control.

## Future work

We investigated the Tsuzuraozaki underwater site in the northern part of Lake Biwa, where many pieces of pottery made during the Jomon and Kofun periods have been discovered. At the site, we operated the developed underwater robot at 50–80 m depth during archaeological non-destructive and non-intrusive surveys. We discovered some pottery (Fig. 1) that had been made after the tenth century. As a next step, we expect to conduct excavation and recovery of archaeological materials. We plan to use the developed robot for underwater excavation. For the recovery of artifacts,

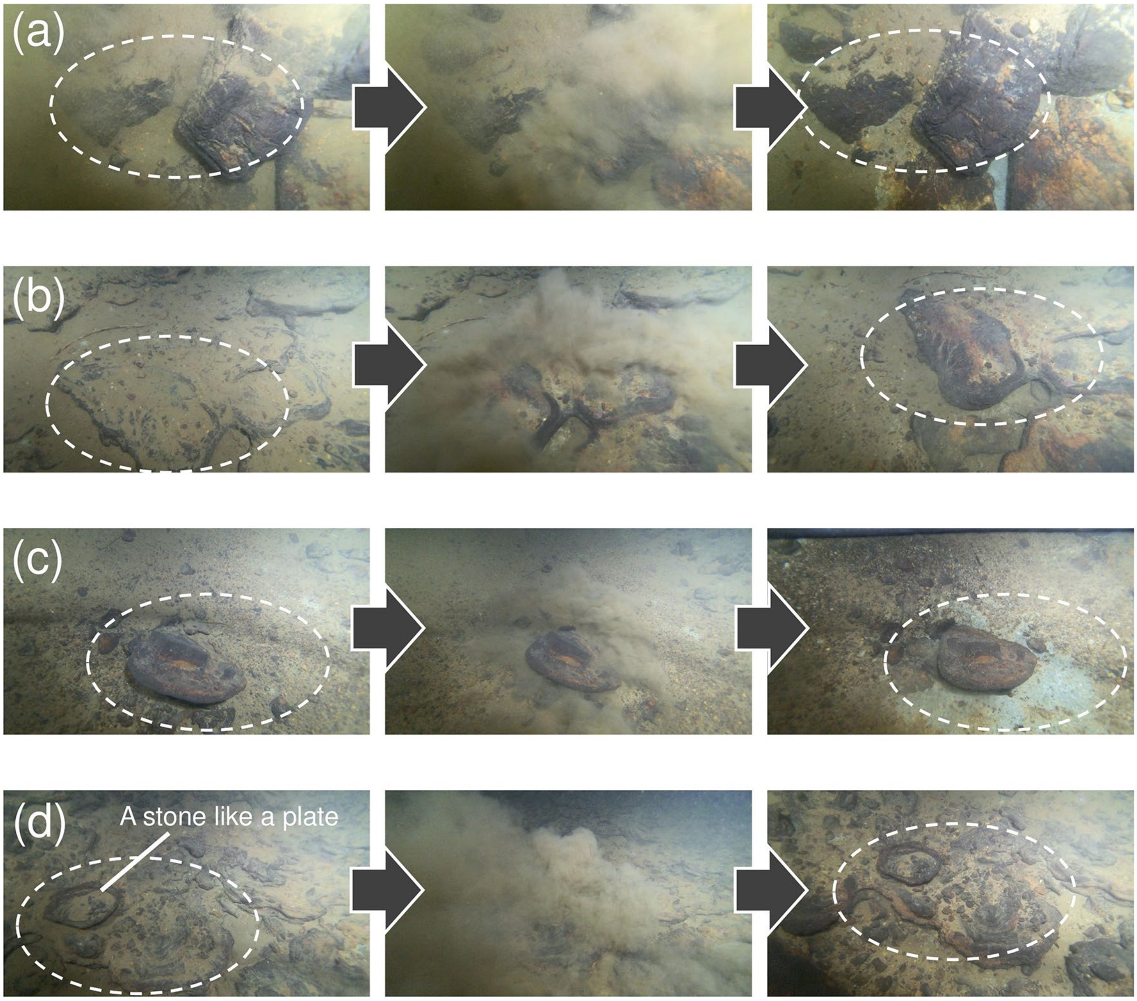

**Fig. 16** Results of sediment removal testing for underwater objects

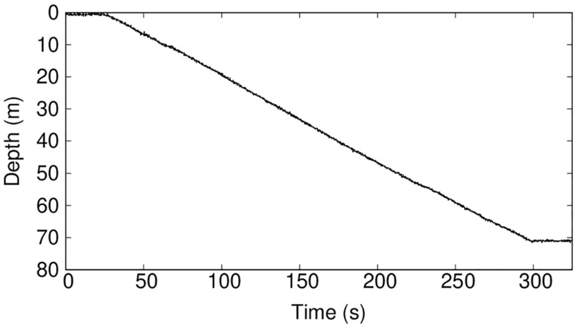

**Fig. 17** Depth data for the robot diving to the lake bottom

it is necessary to design and develop a mechanism for collecting them. Soft mechanisms such as nets and soft robotic grippers are expected to fit the purpose because the artifacts might be fragile. To ensure ease of operations, the robot weight should not be increased by the

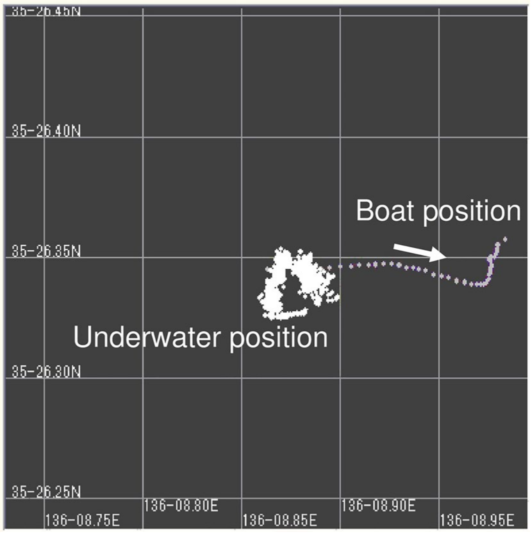

**Fig. 18** Underwater position of the robot at 58 m depth

mounting of a collection mechanism on the robot. Therefore, size and weight reduction of the entire robot are also expected to be extremely important for improving robot functions, including those of the collection mechanisms.

## Conclusion

As described in this paper, we designed, developed, and operated the lightweight underwater robot MIKAN with eight thrusters to investigate underwater archaeological sites. We investigated the potential use of a water flow generated using a pair of small marine thrusters to remove surface sediment for excavation. As described in this paper, we obtained the results described below.

- We conducted preliminary experiments, water flow measurements, and force measurements to determine a thruster configuration that allows our underwater robot to remove sediment in a minimum area of interest.
- Results of preliminary experiments demonstrate that small regular thrusters are useful for sediment removal for excavation.
- We designed and developed the lightweight underwater robot with eight thrusters to conduct archaeological surveys that included underwater excavation.
- Through field experiments, we confirmed that the developed robot with eight thrusters offered good maneuvering performance and sediment removal performance.

From results obtained from a series of the field experiments, we confirmed the usefulness of the developed robot.

### Abbreviations

| | |
|---|---|
| AUV | Autonomous underwater vehicle |
| ROV | Remotely operated vehicle |
| SeRF | Sediment removal and filtration system |

### Acknowledgements

The authors would like to thank Prof. Kenichi Yano (Ritsumeikan University, Japan) for his valuable advice and cooperation in conducting archaeological surveys.

### Author contributions

SH and YM designed and developed the proposed robot, and conducted preliminary and field experiments. NS developed the proposed robot, conducted preliminary experiments and numerical analysis, and drafted the manuscript. MS conducted preliminary experiments. SK contributed to the concept of this study, conducted field experiments, and revised the manuscript. All authors read and approved the final manuscript.

### Funding

This work was supported by a JSPS KAKENHI Grant Number JP15H03271. This work was partially supported by JSPS KAKENHI Grant Number JP21H01294.

### Availability of data and materials

All data generated or analysed during this study are included in this published article.

## Declarations

### Ethics approval and consent to participate

Not applicable.

### Consent for publication

Not applicable.

### Competing interests

The authors declare that they have no competing interests.

Received: 30 October 2022 Accepted: 7 January 2023

### References

1. UNESCO (2013) Objective, methodology and techniques. In: Maarleveld TJ, Guérin U, Egger B (eds.) Manual for Activities Directed at Underwater Cultural Heritage: Guidelines to the Annex of the UNESCO 2001 Convention, pp. 111–126
2. Church RA, Warren DJ, Westrick RF (2010) Reefs, rigs, and wrecks: The 2009 field season of deep-water archaeology in the gulf of mexico. In: Proceedings of 2010 MTS/IEEE OCEANS Seattle, pp. 1–4
3. Gracias N, Ridao P, Garcia R, n JE, L'Hour M, Cibecchini F, Campos R, Carreras M, Ribas D, Palomeras N, Magi L, Palomer A, Nicosevici T, Prados R, Hegedüs R, Neumann L, de Filippo F, Mallios A (2013) Mapping the moon: Using a lightweight auv to survey the site of the 17th century ship 'la lune'. In: Proceedings of 2013 MTS/IEEE OCEANS Bergen, pp. 1–8
4. Allotta B, Costanzi R, Ridolfi A, Reggiannini M, Tampucci M, Scaradozzi D (2016) Archaeology oriented optical acquisitions through marta auv during arrows european project demonstration. In: Proceedings of OCEANS 2016 MTS/IEEE Monterey, pp. 1–4
5. Viswanathan VK, Lobo Z, Lupanow J, von Fock SS, Wood Z, Gambin T, Clark C (2017) Auv motion-planning for photogrammetric reconstruction of marine archaeological sites. In: Proceedings of 2017 IEEE International Conference on Robotics and Automation (ICRA), pp. 5096–5103
6. Nornes SM, Ludvigsen M, Ødegård Ø, Sørensen AJ (2015) Underwater photogrammetric mapping of an intact standing steel wreck with rov. In: IFAC-PapersOnLine, pp. 206–211
7. Drap P, Seinturier J, Hijazi B, Merad D, Boï J-M, Chemisky B, Seguin E, Long L (2015) The rov 3d project: Deep-sea underwater survey using photogrammetry: applications for underwater archaeology. ACM J Comput Cult Herit 8:21–12124
8. Ballard RD, Mccann A, Yoerger DR, Whitcomb LL, Mindell DA, Oleson JP, Singh H, Foley BJ, Adams J, Piechota D, Giangrande C (2000) The discovery of ancient history in the deep sea using advanced deep submergence technology. Deep Sea Res I 47:1591–1620
9. Stemm G, Gerth E, Flow J, Guerra-Librero CL, Kingsley S (2013) The deep-sea tortugas shipwreck, florida: A spanish-operated navio of the 1622 tierra firme fleet. part 2, the artifacts. In: Stemm G, Kingsley S (eds). Oceans Odyssey 3, p. 201. Oxbow Books, Oxford, UK
10. Søreide F, Jasinski M (1998) The unicorn wreck, central Norway: Underwater archaeological investigations of an 18th-century Russian pink, using remotely-controlled equipment. Int J Nautical Archaeol 27:95–112
11. Ballard R, McCann AM, Yoerger D, Whitcomb L, Mindell D, Oleson J, Singh H, Foley B, Adams J, Piechota D, Giangrande C (2000) The discovery of ancient history in the deep sea using advanced deep submergence technology. Deep Sea Res Part I: Oceanographic Res Papers 47:1591–1620
12. Jun B-H, Lee P-M, Jung Y-h (2015) Experience on underwater artefact search using underwater walking robot crabster cr200. In: Proceedings of OCEANS 2015 MTS/IEEE Washington, pp. 1–5
13. Khatib O, Yeh X, Brantner G, Soe B, Kim B, Ganguly S, Stuart H, Wang S, Cutkosky M, Edsinger A, Mullins P, Mitchell Barham CRV, Salama KN,

L'Hour M, Creuze V (2016) Ocean one: A robotic avatar for oceanic discovery. IEEE Robotics Automation Magaz 23:20–29

14. Hannah Stuart SW, Khatib O, Cutkosky MR (2017) The ocean one hands: an adaptive design for robust marine manipulation. Int J Robotics Res 36:150–166
15. Clark CM, Olstad CS, Buhagiar K, Gambin T (2008) Archaeology via underwater robots: Mapping and localization within maltese cistern systems. In: Proceedings of the International Conference on Control, Automation, Robotics and Vision, pp. 662–667
16. Delgado JP, Schwemmer RV (2016) Archaeological survey and identification of uss conestoga (at-54) off southeast farallon island greater farallones national marine sanctuary maritime heritage assessment expedition september 2014-october 2015. In: of National Marine Sanctuaries, O., NOAA (eds.)
17. Green J (2004) Chapter 9. excavation. In: Maritime archaelogy: A Technical Handbook (Second Edition), 2nd edn. Routledge, New York, USA
18. Matsubara M, sakamoto kenji, ohara takuya, fukuda kazuhiro, masuda osamu, kosuge masao (2007) Strength property and fracture toughness of jomon earthenware. In: Proceedings of Conference of Kanto Branch of the Japan Society of Mechanical Engineers, pp. 245–246
19. Hotta S, Mitsui Y, Sakagami N, Kawamura S (2018) Development of a small underwater robot for archaeological survey in fluctuating water-flow environments. In: Proceedings of OCEANS 2018 MTS/IEEE Kobe Techno-Oceans, pp. 1–5

## Publisher's Note

# Terms and Conditions

Springer Nature journal content, brought to you courtesy of Springer Nature Customer Service Center GmbH (“Springer Nature”).

Springer Nature supports a reasonable amount of sharing of research papers by authors, subscribers and authorised users (“Users”), for small-scale personal, non-commercial use provided that all copyright, trade and service marks and other proprietary notices are maintained. By accessing, sharing, receiving or otherwise using the Springer Nature journal content you agree to these terms of use (“Terms”). For these purposes, Springer Nature considers academic use (by researchers and students) to be non-commercial.

These Terms are supplementary and will apply in addition to any applicable website terms and conditions, a relevant site licence or a personal subscription. These Terms will prevail over any conflict or ambiguity with regards to the relevant terms, a site licence or a personal subscription (to the extent of the conflict or ambiguity only). For Creative Commons-licensed articles, the terms of the Creative Commons license used will apply.

We collect and use personal data to provide access to the Springer Nature journal content. We may also use these personal data internally within ResearchGate and Springer Nature and as agreed share it, in an anonymised way, for purposes of tracking, analysis and reporting. We will not otherwise disclose your personal data outside the ResearchGate or the Springer Nature group of companies unless we have your permission as detailed in the Privacy Policy.

While Users may use the Springer Nature journal content for small scale, personal non-commercial use, it is important to note that Users may not:

1. use such content for the purpose of providing other users with access on a regular or large scale basis or as a means to circumvent access control;
2. use such content where to do so would be considered a criminal or statutory offence in any jurisdiction, or gives rise to civil liability, or is otherwise unlawful;
3. falsely or misleadingly imply or suggest endorsement, approval , sponsorship, or association unless explicitly agreed to by Springer Nature in writing;
4. use bots or other automated methods to access the content or redirect messages
5. override any security feature or exclusionary protocol; or
6. share the content in order to create substitute for Springer Nature products or services or a systematic database of Springer Nature journal content.

In line with the restriction against commercial use, Springer Nature does not permit the creation of a product or service that creates revenue, royalties, rent or income from our content or its inclusion as part of a paid for service or for other commercial gain. Springer Nature journal content cannot be used for inter-library loans and librarians may not upload Springer Nature journal content on a large scale into their, or any other, institutional repository.

These terms of use are reviewed regularly and may be amended at any time. Springer Nature is not obligated to publish any information or content on this website and may remove it or features or functionality at our sole discretion, at any time with or without notice. Springer Nature may revoke this licence to you at any time and remove access to any copies of the Springer Nature journal content which have been saved.

To the fullest extent permitted by law, Springer Nature makes no warranties, representations or guarantees to Users, either express or implied with respect to the Springer nature journal content and all parties disclaim and waive any implied warranties or warranties imposed by law, including merchantability or fitness for any particular purpose.

Please note that these rights do not automatically extend to content, data or other material published by Springer Nature that may be licensed from third parties.

If you would like to use or distribute our Springer Nature journal content to a wider audience or on a regular basis or in any other manner not expressly permitted by these Terms, please contact Springer Nature at

onlineservice@springernature.com